Dichomitus squalens partially tailors its molecular responses to the composition of solid wood

Paul Daly [1†], Sara Casado López,[1†] Mao Peng,[1]
Christopher S. Lancefield,[2] Samuel O. Purvine,[3]
Young-Mo Kim,[4] Erika M. Zink,[4] Alice Dohnalkova,[3]
Vasanth R. Singan,[5] Anna Lipzen,[5] David Dilworth,[5]
Mei Wang,[5] Vivian Ng,[5] Errol Robinson,[3] Galya Orr,[3]
Scott E. Baker,[3] Pieter C. A. Bruijnincx,[2]
Kristiina S. Hildén,[6] Igor V. Grigoriev,[5] Miia R. Mäkelä [6]
and Ronald P. de Vries [1,6*]

[1]*Fungal Physiology, Westerdijk Fungal Biodiversity Institute and Fungal Molecular Physiology, Utrecht University, Utrecht, The Netherlands.*

[2]*Inorganic Chemistry and Catalysis, Debye Institute for Nanomaterials Science, Utrecht University, Utrecht, The Netherlands.*

[3]*Environmental Molecular Sciences Laboratory, Pacific Northwest National Laboratory, Richland, WA, USA.*

[4]*Biological Sciences Division, Pacific Northwest National Laboratory, Richland, WA, USA.*

[5]*US Department of Energy Joint Genome Institute, Walnut Creek, CA, USA.*

[6]*Department of Microbiology, University of Helsinki, Helsinki, Finland.*

Summary

White-rot fungi, such as *Dichomitus squalens*, degrade all wood components and inhabit mixed-wood forests containing both soft- and hardwood species. In this study, we evaluated how *D. squalens* responded to the compositional differences in softwood [guaiacyl (G) lignin and higher mannan content] and hardwood [syringyl/guaiacyl (S/G) lignin and higher xylan content] using semi-natural solid cultures. Spruce (softwood) and birch (hardwood) sticks were degraded by *D. squalens* as measured by oxidation of the lignins using 2D-NMR. The fungal response as measured by transcriptomics, proteomics and enzyme activities showed a partial tailoring to wood composition. Mannanolytic transcripts and proteins were more abundant in spruce cultures, while a proportionally higher xylanolytic activity was detected in birch cultures. Both wood types induced manganese peroxidases to a much higher level than laccases, but higher transcript and protein levels of the manganese peroxidases were observed on the G-lignin rich spruce. Overall, the molecular responses demonstrated a stronger adaptation to the spruce rather than birch composition, possibly because *D. squalens* is mainly found degrading softwoods in nature, which supports the ability of the solid wood cultures to reflect the natural environment.

Introduction

White-rot fungi can degrade both wood polysaccharides and lignin by secreting hydrolytic and oxidative enzymes (Floudas *et al*., 2012). *Dichomitus squalens* is a white-rot fungus that in nature is mainly found on softwoods (Andrews and Gill, 1943; Renvall *et al*., 1991), but can also grow on hardwoods (Blanchette *et al*., 1987). Whether white-rot fungi such as *D. squalens* can tailor their molecular responses (i.e., gene expression, protein production and enzymatic activities) to woods of different composition has not been well established. This knowledge could indicate how wood-rotting fungi may adapt to the changes in the diversity of wood species in their environment, for example, by human intervention or global warming. *D. squalens* is found in boreal forest ecosystems (Lindahl *et al*., 2002) that are often mixed forests (EEA-Report, 2006). Climate change may alter which wood types are dominant in these forests and in addition, not only the balance in wood species is likely to change, but possibly also their composition. Understanding this adaptation in a changing climate and knowing whether fungi are able to adapt to these substrate changes is important because degradation of wood by the wood-rotting fungi is a critical contribution to the global carbon cycle (Lindahl *et al*., 2002; Falkowski *et al*., 2008). The analysis of the molecular responses of *D. squalens* to different wood types offers suggestions of whether the fungus could have a fitness advantage as the proportion of wood types in a mixed forest change.

Soft- and hardwood differ in both their polysaccharide (Supporting Information Table S1) and lignin composition. The relative amounts of xylose and mannose reflect the abundance of xylan and mannan in different wood species. The major hemicelluloses in softwood and hardwood are galactoglucomannan and glucuronoxylan, respectively, while each is a minor component in the opposite wood type (Scheller and Ulvskov, 2010). White-rot fungi produce mannanolytic enzymes to degrade galactomannan and xylanolytic enzymes to degrade glucuronoxylan, including enzymes that cleave the side-chain decorations particular to each hemicellulose polymer (Rytioja *et al*., 2014).

Softwood lignin is composed almost entirely of aromatic guaiacyl (G) sub-units, whereas both syringyl (S) and G sub-units are present in hardwood lignin (Ralph *et al*., 2004). White-rot fungi degrade lignin by high redox potential class II heme-peroxidases, that is, lignin, manganese and versatile peroxidases (LiPs, MnPs and VPs), and by laccases (Lundell *et al*., 2014), but there is no evidence for enzyme specificity toward lignin sub-unit composition. Fungi catabolize the wood carbohydrates for energy and growth, while the aromatic breakdown products are mainly converted to less toxic intermediates (Morel *et al*., 2013; Khosravi *et al*., 2015; Mäkelä *et al*., 2015).

Previously, in submerged cultures of *D. squalens* amended with aspen or spruce, no clear tailoring of both the transcriptome and exo-proteome to the wood composition was detected (Rytioja *et al*., 2017). In addition, in previous studies using submerged cultures with other white-rot fungal species *Phanerochaete chrysosporium* (Vanden Wymelenberg *et al*., 2011), *Phanerochaete carnosa* (MacDonald *et al.,* 2011) and *Pycnoporus coccineus* (Miyauchi *et al*., 2017) no compositionally related response to both wood types was reported. In addition, *P. coccineus* also did not adjust its transcriptomes and proteomes to both powdered wood types in solid-state cultures (Couturier *et al*., 2015). As both submerged cultures and powdered wood are significantly different to what white-rot fungi experience in their natural environment, these effects may mask differences in more natural conditions.

The regulatory basis for adaptation to plant biomass composition in wood rotting basidiomycetes is poorly understood as no transcriptional activators of carbohydrate active enzymes (CAZymes) have been characterized. In contrast, the sugar inducers and regulators that adjust the response of various ascomycetes to hemicellulose composition are known [see reviews of Kowalczyk and colleagues (2014); Daly and colleagues (2016); Benocci and colleagues (2017)]. Production of lignin modifying enzymes (LMEs) can be regulated by, for example, carbon and nitrogen concentrations, metals,

and aromatic and xenobiotic compounds (Janusz *et al*., 2013). Recently, Nakazawa and colleagues (2017) identified a transcriptional regulator of LMEs but little otherwise is known of these regulators, and there are none related to lignin sub-unit composition.

D. squalens is a promising reference species for studying wood degradation by white-rot fungi and in addition it also has a potential for biotechnology applications, such as in bioremediation of environmental pollutants (Muzikář *et al*., 2011). The recent establishment of a transformation system (Daly *et al*., 2017) facilitates genetic modification to study the underlying molecular mechanisms of wood decay.

In this study, we explored the ability of *D. squalens* to grow on and degrade wood sticks from a hardwood (birch) and a softwood (spruce) and analysed its molecular responses to the two wood types. Birch and spruce are commonly found in boreal forests and they represent the compositional diversity of wood types (Supporting Information Table S1). We used several complementary techniques, transcriptomics, proteomics and enzyme activity assays, to understand how these woods are modified and whether *D. squalens* tailored its response to wood type compositional differences during cultivation that mimic natural conditions of the fungus.

Results and discussion

D. squalens *degraded both birch and spruce wood sticks over 4-week period*

To mimic natural conditions, *D. squalens* was cultivated on wood sticks over a 4-week period with a visible increase in amount of mycelium (Fig. 1). Helium Ion Microscopy (HIM) demonstrated that after 2 weeks, *D. squalens* had colonized the lumen of the birch and spruce cell walls and there was evidence for wood degradation from thinning of the cell walls in both wood types, especially after 4 weeks (Supporting Information Fig. S1). Thinning of birch wood cell walls by *D. squalens* was observed previously using scanning electron microscopy (SEM) (Blanchette *et al*., 1987) and another analysis at higher magnification suggested a selective degradation strategy when they found a less degraded polysaccharide layer forming around the lumen of poplar (Ruel *et al*., 1994). Using NMR, modification of lignin was detected in both soft- and hardwood (Table 1 and Supporting Information Fig. S2). After 4 weeks, a small but significant increase in the amount of oxidized S units (S′) in birch and G units (G′) in spruce was detected ($p < 0.05$) in the NMR spectra of the whole wood cell walls. Concurrently, a small reduction in the amount of inter-unit lignin bonds (β-O-4, β-β and β-5) was observed in the wood sticks indicating that *D. squalens* may have oxidatively cleaved

Fig. 1. Images of wood-stick cultures of *D. squalens* on spruce or birch at two (2w) and four (4w) weeks.

spruce 2w

birch 2w

spruce 4w

birch 4w

Table 1. Gel-state 2D-HSQC NMR analysis of the lignin and xylan components of wood samples after decay by *D. squalens.*

	Spruce sticks							Birch sticks						
	Non-inoculated controls			*D. squalens* cultures				Non-inoculated controls			*D. squalens* cultures			
Units or bonds	A	B	C	A	B	C	*p* value	A	B	C	A	B	C	*p* value
S	–	–	–	–	–	–	–	62.8	63.6	65.2	55.8	60.3	59.8	0.04
G	96.0	96.9	95.8	94.6	94.6	94.0	0.02	28.0	28.7	27.3	25.5	26	26.1	0.05
S′	–	–	–	–	–	–	–	9.2	7.7	7.5	18.7	13.7	14.1	0.02
G'	4.0	3.1	4.2	5.4	5.4	6.0	0.02	–	–	–	–	–	–	–
β-O-4	34.3	34.1	35.3	31.8	32.4	32.9	0.01	52.6	56.3	54	51.8	44	46.4	0.17
β-β	2.8	2.1	2.3	2.5	1.9	2.2	0.07	4.9	4.6	4.6	4.6	4.0	4.0	0.04
β-5	11.8	11.6	11.5	11.2	11.2	11.2	0.04	2.6	2.3	1.8	2.0	1.9	1.7	0.13
Xi:Xr	31.7	52.4	39.8	26.0	38.5	19.4	0.09	18.8	24.6	21.9	15.3	19.5	21.7	0.18

Gel-state whole cell wall 2D-HSQC NMR analysis of changes in the lignin sub-unit and major inter unit bond composition in spruce and birch sticks after four-week incubation with *D. squalens.* The lignin S/G sub-units are expressed as a percentage of the total units and the inter unit linkages as 'per 100 lignin C9 units'. The abundances of linkages were calculated relative to the S/G units by volume integration of the characteristic a (benzylic) cross peaks in the HSQC spectra, except for the β-O-4 units in birch samples which were quantified using the β cross peak due to overlap of the α cross peak with acetylated xylan residues. The samples are matched pairs where, for example, for spruce the 'A' replicate for the control and that incubated with *D. squalens* were milled concurrently. The *p* value was calculated from a paired two-tailed *t*-test and those with $p < 0.05$ are shaded in grey. S′ = oxidized S units; G' = oxidized G units; Xi:Xr = Xylan internal:Xylan reducing end groups. '–' = below detection limit.

these linkages. Additionally, xylan degradation by *D. squalens* was evaluated by analysing the ratio of xylan internal residues to reducing end groups (Xi:Xr) (Table 1 and Supporting Information Fig. S2). The decrease in this value after fungal growth indicates partial de-polymerization of xylan chains had occurred. Overall, the changes observed by NMR analysis were relatively small, but still significant.

The limited extent of the wood stick degradation may be due to the relatively short cultivation time curtailing the mycelial penetration of the wood combined with the small proportion of the stick surface exposed to the fungus. Limited lignin degradation, as measured by pyrolysis–GC/MS, was also reported from similar solid spruce stick cultures after 6 weeks cultivation of the white-rot fungus *Phlebia radiata* (Kuuskeri *et al*., 2016). Similar to the

D. squalens cultures, the increase in xylan reducing end groups was observed by NMR when the white-rot fungus *Pleurotus ostreatus* was cultivated on small poplar (hardwood) chips (particle size <4 mm) for 3 weeks (Fernández-Fueyo *et al*., 2016). However, no increase in S′ units of lignin was detected. Compared with our study, the shorter cultivation time of *P. ostreatus* could indicate weaker ligninolysis during the early degradation phase, while on the other hand the smaller-sized poplar wood chips may have already been more extensively degraded including release of the S′ units from lignin.

Transcriptomes and extracellular proteomes showed broad-based wood type dependent patterns

With clear evidence for degradation of the wood sticks by *D. squalens*, the molecular responses of the fungus were investigated. The clustering pattern of all expressed transcripts as well as the expressed plant biomass degrading (PBD) CAZy transcripts in a principal component analysis (PCA) demonstrated differences in the responses of *D. squalens* to wood substrates, that is, birch and spruce, as well as to time (Supporting Information Fig. S3). In the exo-proteomes, one of the striking wood type-dependent patterns was an approximately three-fold higher relative abundance of proteins containing a putative signal peptide amongst the total detected proteins in spruce compared with birch cultures at 2 weeks (Supporting Information Table S2A, bottom table). The same trend was also detected in the 4-week cultures. The lower relative abundance of proteins with a signal peptide in birch cultures indicated that there was less signal peptide mediated secretion, more non-classical secretion and/or more proteins released by cell lysis. An indication for the last explanation are the presence of proteins of intracellular metabolism, such as those from the category catabolism (hemicellulosic sugars) in Supporting Information Table S2B. Extracellular proteins of diverse functions have been annotated with a non-classical secretion signal in basidiomycetes although the mechanism of non-classical secretion is not understood (Jain *et al*., 2008; Collins *et al*., 2013). These proteins without a signal peptide were also included in the analysis, as they were potentially part of the natural extracellular response of *D. squalens* to the studied wood substrates. In contrast, in the submerged aspen and spruce cultures of *D. squalens*, the majority of the detected proteins contained a putative signal peptide (Rytioja *et al*., 2017), which may be due to the powdered nature of the substrate and shaken liquid growth system with shorter cultivation times that possibly generates a more uniform culture, while the stick cultures may have more differentiation in the culture, including older and lysing mycelium. Proteins without a putative signal peptide have also been

detected in submerged aspen and pine cultures of *P. chrysosporium*, and they were speculated to originate from cellular lysis (Vanden Wymelenberg *et al*., 2011). The proportion of these proteins increased over time, but no wood type related differences were reported.

Mannan but not xylan degrading CAZy response was tailored to the wood type

D. squalens has a full repertoire of enzymes required to degrade mannan and xylan (Rytioja *et al*., 2014) – the most abundant hemicellulose polysaccharides in spruce and birch, respectively – with 13 mannanolytic CAZymes (MC) and 15 xylanolytic CAZymes (XC) (see Supporting Information Table S3 for full list of activities). Approximately half of the MC transcripts and proteins that were expressed and produced by *D. squalens* positively correlated with the wood composition by being higher in spruce cultivations (Fig. 2A). About a fifth of the MC transcripts and proteins were not induced by either of the wood types under the studied conditions and time points. In contrast to the positive correlation of the MCs, none of the XC transcripts or most of the XC proteins correlated with the wood type as their expression/production was generally higher on spruce (Fig. 2B). Exceptions to this were two β-xylosidases that were detected in higher abundance in the birch cultures at 2 weeks. The correlation between the fold changes in transcript abundance and protein production for the XCs at both time-points were reasonably high ($R^2 > 0.6$) indicating that *D. squalens* was regulating protein levels at least partly if not predominantly by transcription (Fig. 2B). The differences observed between the transcriptome and proteome results are likely due to (a combination of) the time delay between gene expression and protein secretion, the possibility of proteins being bound to the fungal cell wall and therefore not detected in the extracellular fluid, proteolysis resulting in reduced protein levels and possibly other factors, but this did not change the overall pattern observed with both methods. While most of the MC and XC proteins identified were produced at significantly ($p < 0.05$) higher levels on spruce, substantial amounts of these MC and XC proteins were also detected in the birch cultures, in which these proteins still comprised 0.6%–3.6% of the total exo-proteome abundance.

The xylanolytic and mannanolytic activities in the extracellular filtrates of *D. squalens* were measured using a purified xylan and two purified mannans. The ratio of birch xylan to carob galactomannan degrading activity was approximately three-fold higher in the 2-week birch cultures compared with the 2-week spruce cultures (Fig. 3) – a shift which correlates positively with the higher xylan content in birch. A similar shift was not found in the 4-week culture filtrates, as the ratio of the two

Fig. 2. Abundance of CAZy transcripts and proteins involved in the degradation of (A) mannan or (B) xylan. The Pearson correlation (R^2) of $\log_2$ fold changes in transcript (y-axis) or protein (x-axis) abundance is shown adjacent to a particular comparison. Each of the transcripts or proteins in each comparison was categorized according to the colour legend. Abbreviations: 2w(s) and 4w(s) = 2-week and 4-week spruce cultivation, 2w(b) and 4w(b) = 2-week and 4-week birch cultivation, AGL = α-galactosidase, AGU = α-glucuronidase, BXL = β-1,4-xylosidase, GE = glucuronoyl esterase, LPMO = lytic polysaccharide monooxygenase, MAN = β-1,4-endo-mannanase, MND = β-1,4-mannosidase and XLN = β-1,4-endoxylanase.
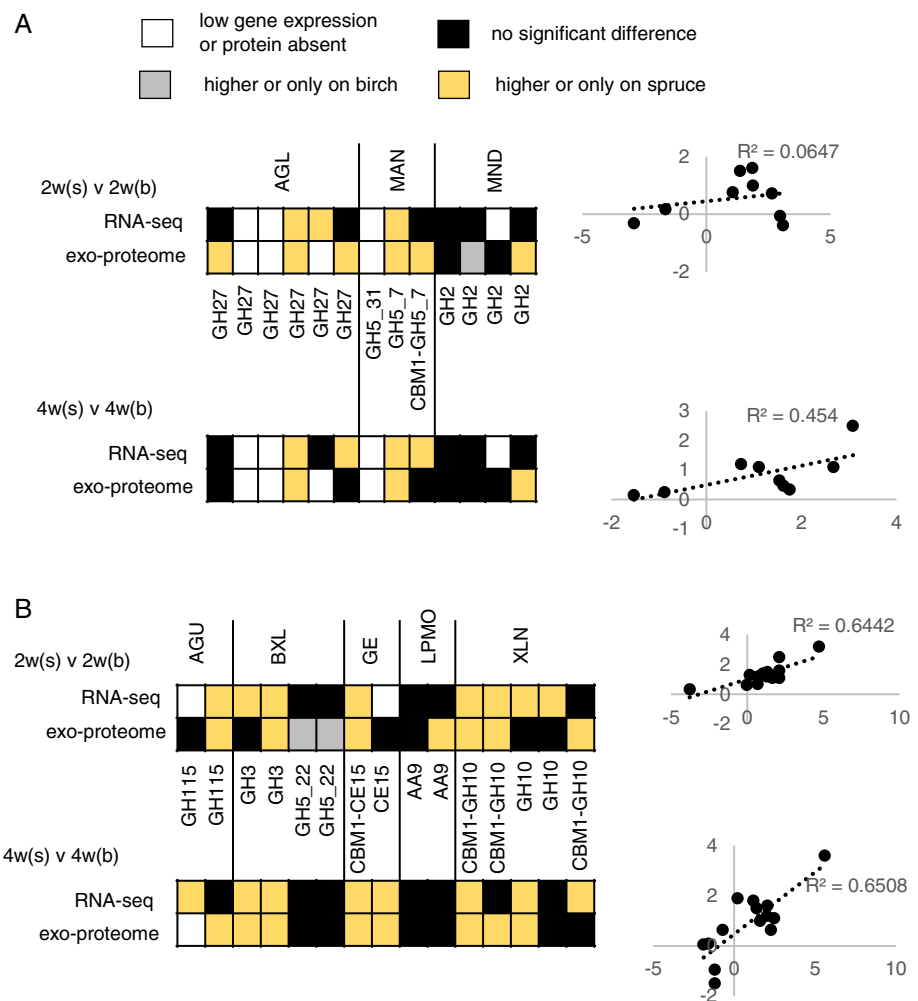

activities in birch and spruce cultures was more variable. In addition, a similar trend was achieved when a galacto-glucomannan purified from spruce instead of commercially available carob storage galactomannan was used as a mannanase substrate (Supporting Information Fig. S4B). In the exo-proteome, in contrast to the proportionally higher xylanolytic activity in the 2-week birch cultures, the abundance of the majority of the endo-xylanase proteins was lower on birch (Fig. 2B). However, the two GH5_22 β-xylosidases with higher abundance in birch cultures at 2 weeks may be contributing to the higher xylan degradation. Previously, low β-xylosidase activity has been reported for *D. squalens* in comparison to other sugar monomer releasing CAZyme activities (Casado López *et al.*, 2017).

The adjustment of the polysaccharide degrading response observed at the gene and protein level was not reflected on the expression of relevant intracellular catabolic enzymes encoding genes (Supporting Information Table S4). Several catabolic pathways have been described in ascomycetes for the sugars that differ in

abundance between birch and spruce (galactose, mannose, xylose and arabinose) (Khosravi *et al.*, 2015). None of the 18 genes identified in *D. squalens* as putatively part of these pathways were differentially expressed between the two wood types in the 2-week cultures. In the 4-week cultures, only two differentially expressed genes were detected, that is, a xylulokinase encoding gene (Dicsqu464_1_PID_821081) with higher expression on spruce cultures and a phosphoglucomutase gene (Dicsqu464_1_PID_951479) with higher expression on birch cultures (Supporting Information Table S4). However, their expression did not correlate with the compositional differences of the wood substrates.

Spruce and birch had an approximately five-fold difference in mannose content, but only a three-fold difference in xylose content (Supporting Information Table S1). The higher mannan content may partly explain the MC response detected in the *D. squalens* spruce cultures. Some differences of xylanolytic activities were detected that positively correlated with the wood composition,
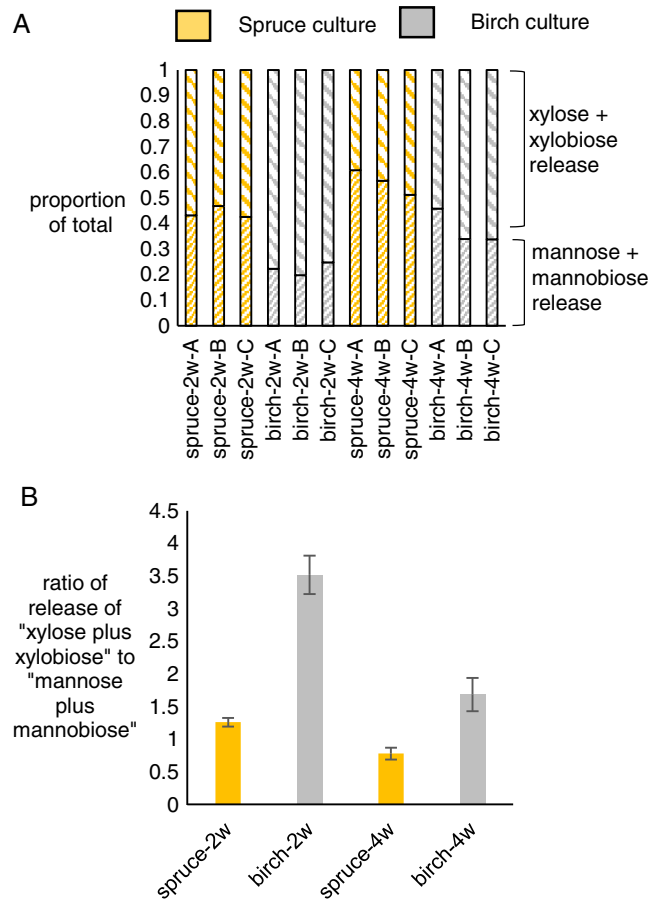
Fig. 3. Extracellular activities of *D. squalens* for degradation of xylan and galactomannan. A. Relative amounts of released sugars from the extracellular filtrates of the three biological replicate cultures toward birchwood xylan (xylose and xylobiose) or carob galactomannan (mannose and mannobiose). B. The ratios to the release of sugars from xylan and galactomannan from the extracellular filtrates. Error bars represent standard errors of biological replicates.

although XC transcript and protein abundance were in general higher in the spruce cultures (Fig. 2B). Small molecule inducers other than those derived from mannan or xylan could be inducing the MCs and XCs in different wood types participating in regulation of gene expression. We recently reported cellobiose as a potent inducer of a broad range of CAZymes, including XCs and MCs, in the same strain of *D. squalens* (Casado López *et al.*, 2018). Cellobiose, which is released during degradation of cellulose, was detected in the exo-metabolomics (Supporting Information Table S5). However, induction by individual sugars can only partially explain induction on crude plant biomass, as multiple sugars are present at varying concentrations.

Some contrasting trends, especially in the respective exo-proteomes than transcriptomes, were detected in the *D. squalens* solid cultures compared with the previous submerged cultures. While a higher subset of MC transcripts was also detected in the submerged spruce cultures, the same trend was not found in the exo-proteome (Rytioja *et al.*, 2017). The spruce cultures had higher XC transcript abundance, but the production of the XC proteins was higher in the aspen cultures, particularly at the earlier time point where most XC proteins were not detected in the spruce cultures (Rytioja *et al.*, 2017). These contrasting trends could be explained by growth differences of *D. squalens* in submerged cultures compared with solid cultures and the use of powdered wood. Other factors such as amount and composition of extractives from birch and aspen may play a role in the response of *D. squalens*, as well as the disruption of the native structure of wood by powdering it before use in submerged cultures. Physiological variability in one fungal strain with respect to a wood species and culturing condition further emphasizes the complexity to compare the results of the other white-rot species from diverse cultivation conditions (MacDonald *et al.*, 2011; Vanden Wymelenberg *et al.*, 2011; Couturier *et al.*, 2015; Miyauchi *et al.*, 2017). Of note however, in *P. coccineus* cultures on powdered wood agar, there was a subset of XC transcripts higher on hardwood (aspen) but no MCs transcripts high on softwood (pine) (Couturier *et al.*, 2015).
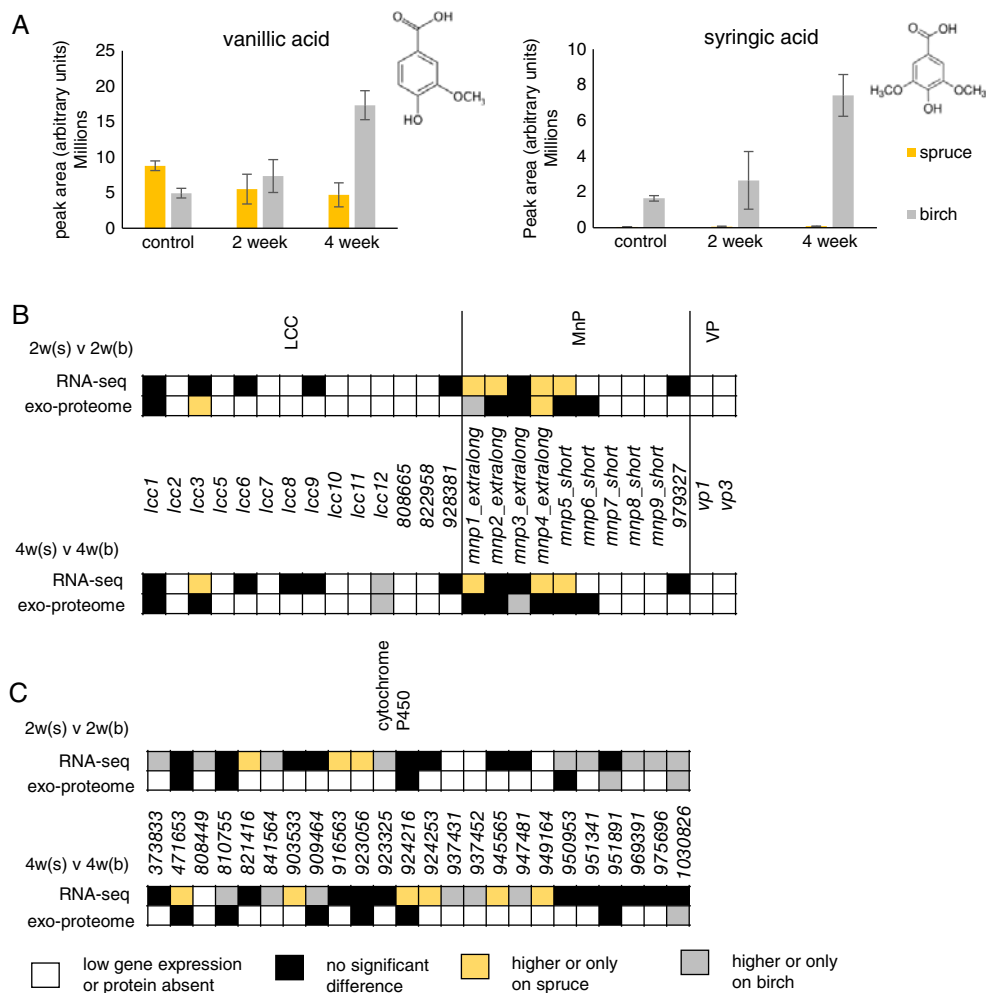
Fig. 4. Lignin degradation related transcript, protein or metabolite abundance. A. Abundance (exo-metabolomics analysis) of two aromatic compounds with the ring methoxylation pattern found in either G or S lignin sub-units. B. Abundance of AA1_1 laccase (LCC) and AA2 manganese peroxidase (MnP) and versatile peroxidase (VP) transcripts and proteins in each of the cross-substrate comparisons. C. Abundance of cytochrome P450 transcripts and proteins that were different in abundance (or only present on one substrate) in either the transcriptome or exo-proteome. Each of the transcripts or proteins in each comparison was categorized according to the colour legend. The gene name or protein ID where no gene name was available is shown. Abbreviations: 2w(s) and 4w(s) = 2-week and 4-week spruce cultivation and 2w(b) and 4w(b) = 2-week and 4-week birch cultivation.

MnPs are the main LMEs induced on solid wood and more so on spruce than birch

In addition to differences in polysaccharide composition, spruce lignin consists almost entirely of G units, while birch lignin is a mixture of S and G units in an approximately 2:1 ratio (Table 1). NMR analysis showed that lignin was oxidized by *D. squalens* during the course of the cultivations (Table 1). Furthermore, in exo-metabolomics, vanillic acid and syringic acid were identified in the *D. squalens* cultures, which are aromatic breakdown products of G and S lignin respectively (Henderson, 1955; Chen *et al*., 1982). In line with the composition of the birch lignin, syringic acid was 50- to 100-fold more abundant in the birch control and cultures (Fig. 4A). However, the abundance of the vanillic acid was similar on

birch and spruce (both controls and cultures) with the largest difference being a four-fold higher level in the birch compared with spruce cultures at 4 weeks. Vanillic acid has been previously identified in the breakdown products from spruce degraded by the white-rot fungus *P. chrysosporium* (Chen *et al*., 1982), while syringic acid has been detected from white-rot degraded birch (Henderson, 1955). The response of *D. squalens* to the birch and spruce lignin was analysed using the transcript and protein abundances of the LMEs and cytochrome P450s (cytP450) that could be metabolizing lignin breakdown products (Morel *et al*., 2013).

D. squalens has 12 putative AA1_1 family laccases and 12 putative AA2 family class II peroxidases of which 10 are manganese peroxidases (MnPs) and two are versatile

peroxidases (VPs) (Rytioja *et al*., 2017) (Fig. 4B). In all cultures, the majority of the laccases were lowly expressed and their corresponding proteins were absent in the exo-proteomes. Furthermore, the overall transcript levels of the laccases were much lower in the solid cultures of our study (< 40 fragments per kilobase of exon model per million reads mapped (FPKM)) than in the previously reported submerged cultures, where several laccases have been highly expressed (> 1000 FPKM) (Rytioja *et al*., 2017). This is corroborated by the exo-proteomes where half as many laccases were identified in the solid cultures compared with those reported from the submerged wood cultures (Rytioja *et al*., 2017). At 4 weeks, one laccase encoding gene (Dicsqu464_1_PID_845680(*lcc12*)) was expressed at a higher level in the birch compared with the spruce cultures and the corresponding protein was only identified in the 4-week birch cultures. Conversely, another laccase (Dicsqu464_1_PID_59186(*lcc3*)) had higher protein abundance in the 2-week spruce compared with birch cultures, while the corresponding transcripts were more abundant after 4 weeks on spruce.

In contrast to laccases, *D. squalens* expressed and produced the majority of the MnPs on the solid wood cultures. Thus, MnPs possibly have a greater role in lignin degradation during the growth of *D. squalens* on solid wood compared with the submerged powdered wood containing cultures (Rytioja *et al*., 2017). The MnP transcript levels were higher on spruce, but the production of two extra-long MnP proteins (Dicsqu464_1_PID_934487 (*mnp1*) and Dicsqu464_1_PID_577408(*mnp3*)) was higher on birch. Both VPs were lowly expressed and the proteins were absent in all cultures. However, a VP (Dicsqu464_1_PID_825366(*vp3*)/Dicsq1_PID_155734) has been identified in the exo-proteome in the submerged spruce and aspen cultures (Rytioja *et al*., 2017). This may indicate that more Mn^{3+} chelates produced by MnPs, which can penetrate the wood structure, are required for lignin degradation in solid wood compared with the powdered wood in the submerged cultures. Furthermore, the higher transcript and protein levels of the MnPs on spruce could be due to a need for greater amounts of Mn^{3+} chelates for degradation of denser G-rich lignin in spruce as was suggested by Couturier and colleagues (2015). There is limited understanding of how wood type affects the LME production. The lack of a pattern of higher transcript and protein abundance of MnPs and VPs on birch may indicate that a tailored LME production is not needed for the degradation of S lignin. In addition, less redox potential is required to oxidize the lignin S units (Ragnar *et al*., 1999) and therefore a smaller subset of the LMEs may be sufficient. The lower expression of the MnP encoding genes on birch could support this hypothesis of a tailoring of the level of redox potential to lignin composition.

D. squalens has 200 putative cytP450 oxidoreductases that are generally located intracellularly and have diverse roles in the conversion of small molecules (Morel *et al*., 2013). The expansion of the number of P450s in wood-rotting fungi was hypothesised to be due to the need for the detoxification of lignin breakdown products (Morel *et al*., 2013). In the 2- and 4-week cultivations of *D. squalens*, 24 cytP450s with differential transcript and/or protein levels were detected (Fig. 4C). Of the 14 that were higher on birch at one or both time points, these were annotated as members of nine cytP450 families. Five of the cytP450 families (CYP512, CYP5035, CYP5037, CYP5144 and CYP5150) were previously found to be enriched in a set of model basidiomycete species and there is evidence for activity from members of these families toward aromatic and flavonoid compounds (Syed *et al*., 2014). Two of the cytP450s were found in higher abundance in the birch exo-proteomes although they likely originate from cellular lysis during the cultivation. The cytP450s with higher gene expression or protein production in the *D. squalens* birch cultures could have a role in metabolizing breakdown products from S-lignin and warrant future analysis of their individual and combinatorial activities toward S-lignin breakdown products. In the *P. coccineus* solid cultures, a small subset of cytP450 genes were also found to be differentially expressed between aspen and pine plate cultures (Couturier *et al*., 2015).

Conclusions

This study expands the understanding of the molecular level responses of white-rot fungi to wood through the use of solid wood stick cultures mimicking their natural growth environment. *D. squalens* partially tailors its molecular responses to wood composition when grown on solid hardwood and softwood sticks. The quantitative rather than qualitative differences in the wood polysaccharides are likely contributing to the limited adjustment detected for the sets of the CAZymes. Other softwoods than spruce with lower xylan content should be analysed to possibly identify a better tailoring of the enzymatic machinery matching to the composition of a hardwood (e.g., Pettersen, 1984) compilation of wood composition highlights several of such softwoods). *D. squalens* is more commonly found on softwoods in nature and this is possibly contributing to the stronger adaptation in the solid cultures to the composition of spruce. This reflection of the natural preference of *D. squalens* for softwood supports the use of the solid cultures to mimic the natural environment. In an increasing spruce-rich forest, *D. squalens* could have a fitness advantage through its higher MC transcripts and protein production on spruce compared with birch but may be at a disadvantage in an

increasingly birch-rich forest. Whether the white-rot fungal responses are adjusted to the qualitative compositional differences in the lignin, requires deeper understanding of the mechanisms of white-rot fungal lignin degradation. Similarly, we cannot exclude that other substances in the different wood types, such as extractives, affect fungal growth and expression of CAZy genes.

Experimental procedures

Growth conditions

The *D. squalens* dikaryotic strain FBCC312 was maintained on 2% (w/v) malt extract 1.5% (w/v) agar (MEA) plates. Static liquid pre-cultures in 250 ml Erlenmeyer flasks containing 50 ml low-nitrogen asparagine-succinate (LN-AS) minimal medium (Hatakka and Uusi-Rauva, 1983), adjusted to pH 4.5 and supplemented with 0.05% (w/v) glycerol, were inoculated with five agar plugs (0.5 cm diameter) and incubated for 7 days at 28°C. The plugs were from fresh fungal mycelium taken from MEA plates, which had been incubated at 28°C. Mycelium from two of the static pre-cultures was fished out with an inoculating loop and transferred to a blender cup that was filled with approximately 50 ml LN-AS medium (without vitamins and glycerol) and blended on a Waring blender for 10 s at 8000 rpm three times with a 30 s pause in between each blending. From the required number of pooled blended pre-cultures, 4 ml was distributed evenly across the surface of each wood stick culture by pipetting. Wood stick cultures were prepared in 250 ml flasks with 100 ml of 1.5% (w/v) water agar. Norway spruce (*Picea abies*) or silver birch (*Betula pendula*) sticks (~ 2 cm length, ~ 0.2 cm width and ~ 0.2 cm height) were autoclaved before transferring 2 g of the sticks onto the set water agar. Triplicate cultures for each time-point (2- and 4-week) and for each set of biomolecule extractions (RNA, exo-proteins and exo-metabolites, and enzyme assays) were incubated at 28°C in the dark.

RNA, protein and metabolite extractions

For RNA extraction, the wood sticks and mycelium were ground using steel chambers with a steel ball in a Tissue-Lyser followed by CsCl gradient ultracentrifugation (Patyshakuliyeva *et al*., 2014). For exo-protein and exo-metabolite extraction, the inoculated sticks (as well as non-inoculated control sticks for exo-metabolites) were transferred to 20 ml of cold water in 100 ml conical flasks and incubated at 4°C and 200 rpm for 2 h. The contents of each of the flasks were filtered through a Büchner funnel fitted with a layer of Miracloth where the filtrate was then frozen in liquid nitrogen, freeze dried and

resolubilized for subsequent separation. Cold 2:1 (v/v) chloroform:methanol was added as a 5:1 (v/v) ratio over the previous collected or extracted samples. The mixture was let stand for 5 min then vortexed for 10 s and centrifuged at 10 000*g* for 10 min at 4°C. The upper aqueous layer was collected for metabolite analysis, while the protein interphase was brought to the bottom of the tube by discarding the lower phase. The protein fraction was then air-dried and stored at −80°C.

RNA library preparation, sequencing and data processing

Plate-based RNA sample preparation was performed on the PerkinElmer Sciclone NGS robotic liquid handling system using Illumina's TruSeq Stranded mRNA HT sample prep kit, which utilizes poly-A selection of mRNA, following the protocol outlined by Illumina in their user guide: http://support.illumina.com/sequencing/sequencing_kits/truseq_stranded_mrna_ht_sample_prep_kit.html. mRNA was purified from 1 μg of total RNA using magnetic beads containing poly-T oligos and was subsequently fragmented and reverse transcribed using random hexamers and SSII (Invitrogen) followed by second strand synthesis. The fragmented cDNA was treated with end-pair, A-tailing, Illumina compatible adapter ligation and eight cycles of PCR was used for library amplification and enrichment. The prepared libraries were quantified using KAPA Biosystem's next-generation sequencing library qPCR kit and run on a Roche LightCycler 480 real-time PCR instrument. The quantified libraries were multiplexed into pools of 12 libraries each, and the pools were prepared for sequencing on the Illumina HiSeq sequencing platform utilizing a TruSeq paired-end cluster kit, v4, and Illumina's cBot instrument to generate a clustered flow cell for sequencing. Sequencing of the flow cell was performed on the Illumina HiSeq2500 sequencer using HiSeq TruSeq SBS sequencing kits, v4, following a 1 × 100 indexed run recipe.

For the read pre-processing, raw fastq file reads were filtered and trimmed using the JGI QC pipeline. Using BBDuk (https://sourceforge.net/projects/bbmap), raw reads were evaluated for artefact sequence by kmer matching (kmer = 25), allowing one mismatch and detected artefact was trimmed from the 3′ end of the reads. RNA spike-in reads, PhiX reads and reads containing any Ns were removed. Quality trimming was performed using the phred trimming method set at Q6. Finally, following trimming, reads under the length threshold were removed (minimum length 25 bases or 1/3 of the original read length – whichever is longer). Filtered reads from each library were aligned to the reference genome (https://genome.jgi.doe.gov/Dicsqu464_1/Dicsqu464_1.home.html) using HISAT version 0.1.4-beta (Kim *et al*., 2015a). FeatureCounts (Liao

et al., 2014) was used to generate the raw gene counts using gff3 annotations. Only primary hits assigned to the reverse strand were included in the raw gene counts (−s 2 −p − primary options). Raw gene counts were used to evaluate the level of correlation between biological replicates using Pearson's correlation (Supporting Information Fig. S5) and determine which replicates would be used in the DGE analysis. DESeq2 (version 1.10.0) (Love *et al.*, 2014) was subsequently used to determine which genes were differentially expressed between pairs of conditions. The parameters used to call a gene DE between conditions were adjusted p value < 0.05. Raw gene counts, not normalized (FPKM) counts were used for DGE analysis as DESeq2 uses its own internal normalization. The reads from each of the RNAseq samples were deposited with the Sequence Read Archive at NCBI with individual sample BioProject Accession numbers (PRJNA411449 to PRJNA411460).

RNAseq data analysis

Genes were considered differentially expressed if the DESeq2 fold change was > 2 or < 0.5 and p_{adj} < 0.05. Genes whose expression was < 10 FPKM were considered lowly expressed and genes whose expression was < 10 FPKM in all four conditions were excluded from analysis. The PCA was performed on the expressed plant biomass degrading CAZy and all expressed genes using FactoMineR version 1.39 (Lê *et al.*, 2008) in R version 3.4.3 where the replicates from a condition clustered together into distinct groupings.

Gene annotations

CAZy (Lombard *et al.*, 2014) annotations for Dicsqu464_1 were from https://genome.jgi.doe.gov/mycocosm/annotations/browser/cazy/summary;VQfPgv?p=Dicsqu464_1. The PBD CAZy were annotated based on Rytioja and colleagues (2017) and updated where required based on the characterized fungal enzymes at http://www.cazy.org/. The PBD subset is listed in Supporting Information Table S3. These PBD CAZy include as well as the polysaccharide degrading CAZymes, the LMEs and other auxiliary activity (AA) enzymes related to lignin degradation. The relevant carbon catabolism genes in *D. squalens* were identified by bidirectional BLAST using the carbon catabolism genes from ascomycetes listed in Patyshakuliyeva and colleagues (2013) or from Khosravi and colleagues (2015) (Supporting Information Table S4). CytP450s were those with the InterPro accession IPR001128 (InterPro accessions were also used for the sub-categories for groups and classes) from the InterProScan (Jones *et al.*, 2014) annotations of the Dicsqu464_1 proteins from the JGI. The CYP family annotations were those assigned to Dicsq1 gene models in the Fungal Cytochrome P450 Database (http://p450.riceblast.snu.ac.kr/index.php?a=view) (Park *et al.*, 2008; Nelson, 2009).

Previous published work on *D. squalens* used the only available *D. squalens* genome annotation (LYAD-421 SS1, Dicsq1), but here for read mapping and peptide matching the annotation of a monokaryotic strain (CBS464.89; Dicsqu464_1) was used. CBS464.89 is a monobasidiospore isolate from the dikaryotic strain FBCC312 (CBS 432.34) (Pham *et al.*, 1990) used for the birch and spruce cultures. To facilitate comparisons with previous *D. squalens* studies, the orthologs between the two *D. squalens* strains (Dicsqu464_1 (https://genome.jgi.doe.gov/Dicsqu464_1/Dicsqu464_1.home.html) and Dicsq1 (http://genome.jgi.doe.gov/Dicsq1/Dicsq1.home.html)) were identified using a bidirectional best hit (BBH) method (Overbeek *et al.*, 1999; Altenhoff and Dessimoz, 2009). The two proteomes were used for all-against-all BLAST searches. Pairs with reciprocal best scores were assigned as putative orthologs and are listed in Supporting Information Table S3.

Proteomic sample preparation and analysis

The protein pellets were dissolved into a solution of 8 M urea in 50 mM NH_4HCO_3 (pH 8.0) with 10% CHAPS and the protein concentration was estimated using a BCA protein assay. The proteins were then denatured and reduced with 5 mM DTT for 30 min at 60°C in a thermomixer. The protein solution was then diluted 10-fold with 50 mM NH_4HCO_3 (pH 8.0), $CaCl_2$ was added at a concentration of 1 mM, and trypsin was added at a ratio of 1:50 enzyme-to-protein prior to incubation for 3 h at 37°C in a thermomixer. The digestion was quenched with a solution of trifluoroacetic acid (1%) before flash freezing and storing at −80°C. The salts and detergents were removed using SCX SPE as described in Kowalczyk and colleagues (2017) and the final peptide concentration was determined using a BCA assay to ensure the samples were diluted to 0.1 $\mu g \cdot \mu l^{-1}$ for LC–MS/MS processing.

All data were collected on a hybrid Velos linear ion trap coupled Orbitrap mass spectrometer (Thermo Electron, Waltham, MA) coupled to a NexGen 3 high performance liquid chromatography system (Agilent Technologies, Santa Clara, CA) through 75 μm × 70 cm columns packed with Phenomenex Jupiter C-18 derivatized 3 μm silica beads (Phenomenex, Torrance, CA). Samples were loaded onto columns with 0.05% formic acid in water and eluted with 0.05% formic acid in acetonitrile over 99 min. Ten data-dependent MS/MS scans were recorded for each survey MS scan using normalized collision energy of 35, isolation width of 2.00, and rolling exclusion window of +1.55/−0.55 Th, lasting 60 s before previously

fragmented signals are eligible for re-analysis. For the MS/MS data search, the MS/MS spectra from all LC–MS/MS datasets were converted to ASCII text (.dta format) using DeconMSn (Mayampurath *et al*., 2008) which more precisely assigns the charge and parent mass values to an MS/MS spectrum. The data files were then interrogated via target-decoy approach (Elias and Gygi, 2010) using MSGFPlus (Kim and Pevzner, 2014) using a ± 20 ppm parent mass tolerance, partially tryptic enzyme settings, and a variable posttranslational modification of oxidized methionine. As part of this processing a target-decoy based Q-value is calculated for each identification within each dataset scaled such that its value roughly reflects the peptide to spectrum match false discovery rate (PSM FDR).

For peptide quantification, MS/MS search results were imported into a Microsoft SQL Server relational database that stores peptide and related protein information, recalculates peptide mass based on IUPAC values, and tracks relative elution times for peptides (Smith *et al*., 2002) normalized between roughly zero and one [Normalized Elution Time (NET); Petritis *et al*., 2006]. Each unique peptide, including post-translational if there are any, is considered a Mass Tag. LC–MS data were deisotoped using Decon2LS (Jaitly *et al*., 2009), and eluting LC–MS features were grouped using MS Feature Finder (Crowell *et al*., 2013) with abundance information for each feature extracted as the sum of monoisotope abundances for each grouped feature. LC–MS features were matched to a filtered list of Mass Tags (≤ 5% PSM FDR via Q-Value) based on mass (± 6 ppm) and NET (± 0.025). Mass and NET tolerances were dynamically refined based on histogram width. False matching events between Mass Tags and LC–MS features were controlled via STAC score ≥ 0.60 (~6% FDR, Stanley *et al*., 2011) and the final list of all Mass Tags and their related abundance values combined across all data and exported to Microsoft Excel.

Only peptides that were a match to a single protein (i.e., unique peptides) from Dicsqu464_1 were used for subsequent analysis. The peptide abundance values were summed to the protein level and then the protein abundance values were normalized to adjust for differences in total abundance by adjusting the values in a sample so that every sample had the same mean abundance value. For a protein to be considered identified, the requirements were a minimum of two peptides (unique to that protein) identified in the dataset and an abundance measurement in at least two of the replicates for that condition. For an identified protein to be considered significantly different in abundance, the requirements were a two-fold change of the mean abundance values and $p < 0.05$ from a two-tailed heteroscedastic (assuming unequal variances) *t*-test of the $\log_2$ transformed abundance values. Proteins were categorized as higher (or only present) in the birch or spruce cultures, not significantly different or not present. Proteins considered to be conventionally secreted were those with a SignalP (Petersen *et al*., 2011) HMM probability (hmm_signalpep_probability) > 0.5 using the annotations from https://genome.jgi.doe.gov/Dicsqu464_1/Dicsqu464_1.home.html. For the analysis of cytP450s, a higher five-fold change in abundance threshold, only considering cytP450s that were identified in both of the wood type cultures was used to control artefacts caused by possible differences in the levels of cellular lysis in the cultures.

Metabolomics

Metabolomics analysis was performed as reported previously (Khosravi *et al*., 2018). Extracted metabolites were completely dried under speed-vacuum and chemically derivatized as reported previously (Kim *et al*., 2015b). Briefly, equivalent volumes of the extracted metabolites from all samples were derivatized by methoxyamination and trimethylsilyation (TMS), then the samples were analysed by GC–MS. GC–MS raw data files were processed using the Metabolite Detector software, version 2.5 beta (Hiller *et al*., 2009). Briefly, original data files were converted to netCDF format using vendor's software, followed by conversion to binary files using Metabolite Detector. Retention indices of detected metabolites were calculated based on analysis of the fatty acid methyl esters mixture (C8–C28), followed by chromatographic alignment across all analyses after de-convolution. Metabolites were initially identified by matching experimental spectra to an in-house GC–MS metabolomics database, containing spectra and validated retention indices for over 850 metabolites, then unknown peaks were additionally matched with the NIST14 GC–MS library. All metabolite identifications were validated to reduce deconvolution errors during automated data-processing and to eliminate false identifications.

Enzyme assays with mannan and xylan polysaccharides

For enzyme assays, the extracellular proteins were collected from triplicate two-week and four-week cultures as described previously. However, the filtrate, instead of freeze drying, was centrifuged at 3220*g*, 4°C for 10 min to pellet any solids before concentrating the supernatant approximately 10-fold using Vivaspin (GE Life Sciences) columns with a 5000 molecular weight cut-off by centrifuging at 4°C and 3220*g*. Enzyme assays were performed in 96-well plates in a total volume of 200 μl, containing 50 mM sodium acetate buffer pH 5, with shaking at 600 rpm on a plate shaker at 40°C for 16 h. As substrates, 0.5% (w/v) concentration of galactomannan (carob) (Megazyme), galactoglucomannan from spruce prepared according to Andersson and colleagues (2007)

or birchwood xylan (Sigma) were used. The reactions were terminated by heating at 99°C for 5 min. Enzymatic reactions were performed in duplicate in the 96-well plate and were pooled for measurement of the sugars released (xylose, xylobiose, mannose and mannobiose) using a Dionex HPAEC-PAD (Dionex ICS-5000+ system; Thermo Scientific) system with the program for measuring the monosaccharides as Mäkelä and colleagues (2016) and the program for the disaccharides as Mäkelä and colleagues (2018). About 5–250 μM xylobiose and mannobiose (Megazyme) were used as standards for measuring the disaccharides. Controls without substrate or filtrate were also performed. Volumes of each of the extracellular filtrates were assayed in a range where a particular sugar could be measured when the release was increasing (i.e*., not plateaued) [mannobiose (2.5 and 5 μl), mannose (5 and 10 μl), xylobiose (0.25 and 1 μl) and xylose (10 μl)]. Based on the amounts of monomers and dimers released, not more than approximately 10% of the polysaccharides had been saccharified. The μmol amount of a sugar released in a reaction was expressed per volume of filtrate. The μmol μl^{-1} release of the respective monomers and dimers were summed (i.e., mannose plus mannobiose and xylose plus xylobiose) and the ratio of the respective monomer plus dimer release from each filtrate was calculated to indicate changes in the relative proportions of mannan and xylan degrading activities in the extracellular filtrate. The calculation of this ratio aided in controlling for varying levels of total secreted protein, cellular lysis and proteolysis in different solid-state cultures.

NMR analysis

The wood sticks from the 4-week cultures for NMR analysis were collected as by the method for extracellular proteins whereby the sticks that were captured by the Büchner funnel were air-dried in a 60°C oven for 7 days. Triplicate non-inoculated control cultures were incubated under the same conditions as the fungal cultures. NMR analysis was performed following Kim and Ralph (2010). Briefly, air-dried wood sticks were manually reduced to approximately < 5 mm in all dimensions using scissors. Approximately 400–500 mg of this material was then placed in a 50 ml centrifuge tube and extracted sequentially with water (2 × 40 ml), 80% ethanol (2 × 40 ml) and acetone (2 × 40 ml) by ultrasonication for 30 min, with the supernatant being removed by decantation each time. The extractive free wood chips were allowed to air dry (24 h) before a 250 mg portion was finely milled in a planetary ball mill for 15 h using a 50 ml agate jar containing 1 × 20 mm, 1 × 15 mm and 6 × 10 mm agate balls. The samples were milled using a 'vintage style' Fritsch 'Pulverisette 7' mill at speed setting 7.5. Under

these conditions sample heating was negligible. Approximately 70 mg of milled cell wall material was transferred directly to a 5 mm NMR tube and evenly distributed up the sides of the tube (bottom ~ 5 cm). About 600 μl of premixed d_6-DMSO:d_5-Pyrdine (4:1) solution was then carefully introduced directly to the bottom of the tube using a long needle and syringe. The sample was mixed by vigorous shaking followed by ultrasonication for 30 min forming a uniform gel.

NMR spectra were acquired on a 6000 MHz Bruker Advance II spectrometer equipped with a ^{1}H-^{13}C/^{15}N/^{2}H CPTCI Cryoprobe. 2D ^{1}H–^{13}C HSQC spectra were acquired using a standard Bruker pulse program (hsqcetgpsisp2). The NMR spectra were acquired from 13 to −1 ppm in F2 (^{1}H) using 2048 data points for an acquisition time (AQ) of 122 ms, an interscan delay (D1) of 1 s, 47–137 ppm in F1 (^{13}C) using 144 increments and 64 scans. The spectrum was processed using squared cosinebell in both dimensions and LPfc linear prediction (18 coefficients) in F1. Interactive integrations of contours in 2D HSQC plots were carried out using Bruker's TopSpin 3.5 (Windows) software, as was all data processing. Lignin and carbohydrate assignments were made based on literature reports (Kim and Ralph, 2010, 2014; Johnson *et al*., 2017).

Semi-quantitative analysis of the lignin components was accomplished by integration and comparison of the $S_{2/6}$ and G_2 resonances in the aromatic region and the characteristic signals for each structural unit in the oxygenated alkyl region. Abundances of the lignin linkages are expressed as the number of linkages per 100 C_9 units. Relative amounts of hemicellulose components were calculated by a similar comparison of the integrals using the anomeric carbohydrate resonances as a reference. Figures were produced using Adobe Illustrator. A two-tailed paired *t*-test was used to determine significant differences in the NMR data.

Microscopy sample preparation and imaging

Interactions of fungal hyphae and wood cells were analysed by Helium Ion microscopy (HIM). Three representatives of mycelium-wood sticks from every flask were inspected and the images taken were representative of their entire (respective) sample. The mycelium-wood stick was fully submerged in glutaraldehyde 2.5% to fix it and preserved at 4°C until processed. The wood sticks were dissected with a scalpel to the dimensions of approximately 1 × 2 × 2 mm, washed three times in 1% phosphate-buffered saline (PBS), and gradually dehydrated in an ethanol series (25%, 33%, 50%, 75% and three times at 100%, 15 min each). The samples were then placed in the chamber of a critical point dryer (CPD) (Tousimis, Autosamdri – 815) and processed according

to an automated CPD scheme, with CO_2 as a transitional fluid. The samples were then mounted on standard carbon tape-covered aluminium SEM stubs (Ted Pella, Redding, CA), and sputter-coated with carbon. The samples were imaged with a high-resolution Orion Helium ion microscope, (Zeiss, Peabody, MA) at 30 keV.

Author contributions

RPdV, MRM and KSH devised the solid cultures experiment. PD and SCL performed experiments and wrote the manuscript. MP performed bioinformatic analysis. YMK and EMZ performed metabolomics analysis. SOP and EMZ performed proteomics analysis. AD performed microscopic analysis. DD, MW, AL and VRS generated and processed the RNAseq dataset at the JGI where IVG and VN coordinated this work. GO, ER and SEB coordinated the work at EMSL. CSL and PCAB devised the NMR experiments and CSL generated and analysed the NMR dataset.

References

Altenhoff, A. M., and Dessimoz, C. (2009) Phylogenetic and functional assessment of orthologs inference projects and methods. *PLoS Comp Biol* **5**: e1000262.

Andersson, A., Persson, T., Zacchi, G., Stålbrand, H., and Jönsson, A.-S. (2007) Comparison of diafiltration and size-exclusion chromatography to recover hemicelluloses from process water from thermomechanical pulping of spruce. In *Applied Biochemistry and Biotecnology: The Twenty-Eighth Symposium Proceedings of the Twenty-Eight Symposium on Biotechnology for Fuels and Chemicals Held April 30–May 3, 2006, in Nashville, Tennessee*, Mielenz, J. R., Klasson, K. T.,

Adney, W. S., and McMillan, J. D. (eds). Totowa, NJ: Humana Press, pp. 971–983.

Andrews, S. R., and Gill, L. S. (1943) Western red rot in immature ponderosa pine in the southwest. *J Forest* **41**: 565–573.

Benocci, T., Aguilar-Pontes, M. V., Zhou, M., Seiboth, B., and de Vries, R. P. (2017) Regulators of plant biomass degradation in ascomycetous fungi. *Biotechnol Biofuels* **10**: 152.

Blanchette, R., Otjen, L., and Carlson, M. (1987) Lignin distribution in cell walls of birch wood decayed by white rot basidiomycetes. *Phytopathology* **77**: 684–690.

Casado López, S., Peng, M., Issak, T. Y., Daly, P., de Vries, R. P., and Mäkelä, M. R. (2018) Induction of genes encoding plant cell wall-degrading carbohydrate-active enzymes by lignocellulose-derived monosaccharides and cellobiose in the white-rot fungus *Dichomitus squalens*. *Appl Environ Microbiol* **84**: e00403–e00418.

Casado López, S., Theelen, B., Manserra, S., Issak, T. Y., Rytioja, J., Mäkelä, M. R., and de Vries, R. P. (2017) Functional diversity in *Dichomitus squalens* monokaryons. *IMA Fungus* **8**: 17–25.

Chen, C.-L., Chang, H.-M., and Kirk, T. K. (1982) Aromatic acids produced during degradation of lignin in spruce wood by *Phanerochaete chrysosporium*. *Holzforschung* **36**: 3–9.

Collins, C., Keane, T. M., Turner, D. J., O'Keeffe, G., Fitzpatrick, D. A., and Doyle, S. (2013) Genomic and proteomic dissection of the ubiquitous plant pathogen, *Armillaria mellea*: toward a new infection model system. *J Proteome Res* **12**: 2552–2570.

Couturier, M., Navarro, D., Chevret, D., Henrissat, B., Piumi, F., Ruiz-Dueñas, F. J., *et al*. (2015) Enhanced degradation of softwood versus hardwood by the white-rot fungus *Pycnoporus coccineus*. *Biotechnol Biofuels* **8**: 1–16.

Crowell, K. L., Slysz, G. W., Baker, E. S., LaMarche, B. L., Monroe, M. E., Ibrahim, Y. M., *et al*. (2013) LC-IMS-MS feature finder: detecting multidimensional liquid chromatography, ion mobility and mass spectrometry features in complex datasets. *Bioinformatics* **29**: 2804–2805.

Daly, P., van Munster, J. M., Raulo, R., and Archer, D. B. (2016) Transcriptional regulation and responses in filamentous fungi exposed to lignocellulose. In *Fungal Biotechnology for Biofuel Production*, Silva, R. (ed). Sharjah, UAE: Benthan ebooks, pp. 82–127.

Daly, P., Slaghek, G. G., Casado López, S., Wiebenga, A., Hildén, K. S., de Vries, R. P., and Mäkelä, M. R. (2017) Genetic transformation of the white-rot fungus *Dichomitus squalens* using a new commercial protoplasting cocktail. *J Microbiol Methods* **143**: 38–43.

EEA-Report (2006) European Environment Agency Technical Report: the European forest types — Categories and types for sustainable forest management reporting and policy. In *Technical report No 9/2006*.

Elias, J. E., and Gygi, S. P. (2010) Target-decoy search strategy for mass spectrometry-based proteomics. *Methods Mol Biol* **604**: 55–71.

Falkowski, P. G., Fenchel, T., and Delong, E. F. (2008) The microbial engines that drive Earth's biogeochemical cycles. *Science* **320**: 1034–1039.

Fernández-Fueyo, E., Ruiz-Dueñas, F. J., López-Lucendo, M. F., Pérez-Boada, M., Rencoret, J., Gutiérrez, A., *et al*. (2016) A secretomic view of woody and nonwoody lignocellulose degradation by *Pleurotus ostreatus*. *Biotechnol Biofuels* **9**: 49.

Floudas, D., Binder, M., Riley, R., Barry, K., Blanchette, R. A., Henrissat, B., *et al*. (2012) The paleozoic origin of enzymatic lignin decomposition reconstructed from 31 fungal genomes. *Science* **336**: 1715–1719.

Hatakka, A. I., and Uusi-Rauva, A. K. (1983) Degradation of ^{14}C-labelled poplar wood lignin by selected white-rot fungi. *Appl Microbiol Biotechnol* **17**: 235–242.

Henderson, M. E. K. (1955) Release of aromatic compounds from birch and spruce sawdusts during decomposition by white-rot fungi. *Nature* **175**: 634–635.

Hiller, K., Hangebrauk, J., Jager, C., Spura, J., Schreiber, K., and Schomburg, D. (2009) MetaboliteDetector: comprehensive analysis tool for targeted and nontargeted GC/MS based metabolome analysis. *Anal Chem* **81**: 3429–3439.

Jain, P., Podila, G. K., and Davis, M. R. (2008) Comparative analysis of non-classically secreted proteins in *Botrytis cinerea* and symbiotic fungus *Laccaria bicolor*. *BMC Bioinform* **9**: O3.

Jaitly, N., Mayampurath, A., Littlefield, K., Adkins, J. N., Anderson, G. A., and Smith, R. D. (2009) Decon2LS: an open-source software package for automated processing and visualization of high resolution mass spectrometry data. *BMC Bioinform* **10**: 87.

Janusz, G., Kucharzyk, K. H., Pawlik, A., Staszczak, M., and Paszczynski, A. J. (2013) Fungal laccase, manganese peroxidase and lignin peroxidase: gene expression and regulation. *Enzyme Microb Technol* **52**: 1–12.

Johnson, A. M., Kim, H., Ralph, J., and Mansfield, S. D. (2017) Natural acetylation impacts carbohydrate recovery during deconstruction of *Populus trichocarpa* wood. *Biotechnol Biofuels* **10**: 48.

Jones, P., Binns, D., Chang, H. Y., Fraser, M., Li, W., McAnulla, C., *et al*. (2014) InterProScan 5: genome-scale protein function classification. *Bioinformatics* **30**: 1236–1240.

Khosravi, C., Benocci, T., Battaglia, E., Benoit, I., and de Vries, R. P. (2015) Sugar catabolism in *Aspergillus* and other fungi related to the utilization of plant biomass. *Adv Appl Microbiol* **90**: 1–28.

Khosravi, C., Battaglia, E., Kun, R. S., Dalhuijsen, S., Visser, J., Aguilar-Pontes, M. V., *et al*. (2018) Blocking hexose entry into glycolysis activates alternative metabolic conversion of these sugars and upregulates pentose metabolism in *Aspergillus nidulans*. *BMC Genom* **19**: 214.

Kim, D., Langmead, B., and Salzberg, S. L. (2015a) HISAT: a fast spliced aligner with low memory requirements. *Nat Methods* **12**: 357–360.

Kim, H., and Ralph, J. (2010) Solution-state 2D NMR of ball-milled plant cell wall gels in DMSO-d6/pyridine-d5. *Org Biomol Chem* **8**: 576–591.

Kim, H., and Ralph, J. (2014) A gel-state 2D-NMR method for plant cell wall profiling and analysis: a model study with the amorphous cellulose and xylan from ball-milled cotton linters. *RSC Adv* **4**: 7549–7560.

Kim, S., and Pevzner, P. A. (2014) MS-GF+ makes progress towards a universal database search tool for proteomics. *Nat Commun* **5**: 5277.

Kim, Y. M., Nowack, S., Olsen, M. T., Becraft, E. D., Wood, J. M., Thiel, V., *et al*. (2015b) Diel metabolomics analysis of a hot spring chlorophototrophic microbial mat leads to new hypotheses of community member metabolisms. *Front Microbiol* **6**: 209.

Kowalczyk, J. E., Benoit, I., and de Vries, R. P. (2014) Regulation of plant biomass utilization in *Aspergillus*. *Adv Appl Microbiol* **88**: 31–56.

Kowalczyk, J. E., Khosravi, C., Purvine, S., Dohnalkova, A., Chrisler, W. B., Orr, G., *et al*. (2017) High resolution visualization and exo-proteomics reveal the physiological role of XlnR and AraR in plant biomass colonization and degradation by *Aspergillus niger*. *Environ Microbiol* **19**: 4587–4598.

Kuuskeri, J., Häkkinen, M., Laine, P., Smolander, O.-P., Tamene, F., Miettinen, S., *et al*. (2016) Time-scale dynamics of proteome and transcriptome of the white-rot fungus *Phlebia radiata*: growth on spruce wood and decay effect on lignocellulose. *Biotechnol Biofuels* **9**: 1–22.

Lê, S., Josse, J., and Husson, F. (2008) FactoMineR: an R package for multivariate analysis. *J Stat Softw* **25**: 18.

Liao, Y., Smyth, G. K., and Shi, W. (2014) featureCounts: an efficient general purpose program for assigning sequence reads to genomic features. *Bioinformatics* **30**: 923–930.

Lindahl, B. O., Taylor, A. F. S., and Finlay, R. D. (2002) Defining nutritional constraints on carbon cycling in boreal forests – towards a less `phytocentric' perspective. *Plant Soil* **242**: 123–135.

Lombard, V., Golaconda Ramulu, H., Drula, E., Coutinho, P. M., and Henrissat, B. (2014) The carbohydrate-active enzymes database (CAZy) in 2013. *Nucleic Acids Res* **42**: D490–D495.

Love, M., Huber, W., and Anders, S. (2014) Moderated estimation of fold change and dispersion for RNA-seq data with DESeq2. *Genome Biol* **15**: 550.

Lundell, T. K., Mäkelä, M. R., de Vries, R. P., and Hildén, K. S. (2014) Genomics, lifestyles and future prospects of wood-decay and litter-decomposing basidiomycota. *Adv Bot Res* **70**: 329–370.

MacDonald, J., Doering, M., Canam, T., Gong, Y., Guttman, D. S., Campbell, M. M., and Master, E. R. (2011) Transcriptomic responses of the softwood-degrading white-rot fungus *Phanerochaete carnosa* during growth on coniferous and deciduous wood. *Appl Environ Microbiol* **77**: 3211–3218.

Mäkelä, M. R., Mansouri, S., Wiebenga, A., Rytioja, J., de Vries, R. P., and Hildén, K. S. (2016) *Penicillium subrubescens* is a promising alternative for *Aspergillus niger* in enzymatic plant biomass saccharification. *New Biotechnol* **33**: 834–841.

Mäkelä, M. R., Dilokpimol, A., Koskela, S. M., Kuuskeri, J., de Vries, R. P., and Hildén, K. (2018) Characterization of a feruloyl esterase from *Aspergillus terreus* facilitates the division of fungal enzymes from carbohydrate esterase family 1 of the carbohydrate-active enzymes (CAZy) database. *Microbial Biotechnol* **11**: 869–880.

Mäkelä, M. R., Marinović, M., Nousiainen, P., Liwanag, A. J. M., Benoit, I., Sipilä, J., *et al*. (2015) Aromatic metabolism of

filamentous fungi in relation to the presence of aromatic compounds in plant biomass. *Adv Appl Microbiol* **91**: 63–137.

Mayampurath, A. M., Jaitly, N., Purvine, S. O., Monroe, M. E., Auberry, K. J., Adkins, J. N., and Smith, R. D. (2008) DeconMSn: a software tool for accurate parent ion monoisotopic mass determination for tandem mass spectra. *Bioinformatics* **24**: 1021–1023.

Miyauchi, S., Navarro, D., Grisel, S., Chevret, D., Berrin, J.-G., and Rosso, M.-N. (2017) The integrative omics of white-rot fungus *Pycnoporus coccineus* reveals co-regulated CAZymes for orchestrated lignocellulose breakdown. *PLoS One* **12**: e0175528.

Morel, M., Meux, E., Mathieu, Y., Thuillier, A., Chibani, K., Harvengt, L., *et al*. (2013) Xenomic networks variability and adaptation traits in wood decaying fungi. *J Microb Biotechnol* **6**: 248–263.

Muzikář, M., Křesinová, Z., Svobodová, K., Filipová, A., Čvančarová, M., Cajthamlová, K., and Cajthaml, T. (2011) Biodegradation of chlorobenzoic acids by ligninolytic fungi. *J Hazard Mater* **196**: 386–394.

Nakazawa, T., Izuno, A., Kodera, R., Miyazaki, Y., Sakamoto, M., Isagi, Y., and Honda, Y. (2017) Identification of two mutations that cause defects in the ligninolytic system through an efficient forward genetics in the white-rot agaricomycete *Pleurotus ostreatus*. *Environ Microbiol* **9**: 261–272.

Nelson, D. R. (2009) The cytochrome P450 homepage. *Hum Genom* **4**: 59–65.

Overbeek, R., Fonstein, M., D'Souza, M., Pusch, G. D., and Maltsev, N. (1999) The use of gene clusters to infer functional coupling. *Proc Natl Acad Sci USA* **96**: 2896–2901.

Park, J., Lee, S., Choi, J., Ahn, K., Park, B., Park, J., *et al*. (2008) Fungal cytochrome P450 database. *BMC Genom* **9**: 402–402.

Patyshakuliyeva, A., Mäkelä, M. R., Sietiö, O.-M., de Vries, R. P., and Hildén, K. S. (2014) An improved and reproducible protocol for the extraction of high quality fungal RNA from plant biomass substrates. *Fungal Genet Biol* **72**: 201–206.

Patyshakuliyeva, A., Jurak, E., Kohler, A., Baker, A., Battaglia, E., de Bruijn, W., *et al*. (2013) Carbohydrate utilization and metabolism is highly differentiated in *Agaricus bisporus*. *BMC Genom* **14**: 663.

Petersen, T. N., Brunak, S., Heijne, G., and Nielsen, H. (2011) SignalP 4.0: discriminating signal peptides from transmembrane regions. *Nat Methods* **8**: 785–786.

Petritis, K., Kangas, L. J., Yan, B., Monroe, M. E., Strittmatter, E. F., Qian, W. J., *et al*. (2006) Improved peptide elution time prediction for reversed-phase liquid chromatography-MS by incorporating peptide sequence information. *Anal Chem* **78**: 5026–5039.

Pettersen, R. C. (1984) The chemical composition of wood . In *The Chemistry of Solid Wood*, Rowell, R. M. (ed). Washington, DC: American Chemical Society, pp. 57–126.

Pham, T. T. T., Maaroufi, A., and Odier, E. (1990) Inheritance of cellulose- and lignin-degrading ability as well as endoglucanase isozyme pattern in *Dichomitus squalens*. *Appl Microbiol Biotechnol* **33**: 99–104.

Ragnar, M., Eriksson, T., and Reitberger, T. (1999) Radical formation in ozone reactions with lignin and carbohydrate model compounds. *Holzforschung* **53**: 292–298.

Ralph, J., Lundquist, K., Brunow, G., Lu, F., Kim, H., Schatz, P. F., *et al*. (2004) Lignins: natural polymers from oxidative coupling of 4-hydroxyphenyl- propanoids. *Phytochem Rev* **3**: 29–60.

Renvall, P., Renvall, T., and Niemelä, T. (1991) Basidiomycetes at the timberline in Lapland 2. An annotated checklist of the polypores of northeastern Finland. *Karstenia* **31**: 13–28.

Ruel, K., Ambert, K., and Joseleau, J.-P. (1994) Influence of the enzyme equipment of white-rot fungi on the patterns of wood degradation. *FEMS Microbiol Rev* **13**: 241–254.

Rytioja, J., Hildén, K., Yuzon, J., Hatakka, A., de Vries, R. P., and Mäkelä, M. R. (2014) Plant-polysaccharide-degrading enzymes from basidiomycetes. *Microbiol Mol Biol Rev* **78**: 614–649.

Rytioja, J., Hildén, K., Di Falco, M., Zhou, M., Aguilar-Pontes, M. V., Sietiö, O.-M., *et al*. (2017) The molecular response of the white-rot fungus *Dichomitus squalens* to wood and non-woody biomass as examined by transcriptome and exoproteome analyses. *Environ Microbiol* **19**: 1237–1250.

Scheller, H. V., and Ulvskov, P. (2010) Hemicelluloses. *Annu Rev Plant Biol* **61**: 263–289.

Smith, R. D., Anderson, G. A., Lipton, M. S., Pasa-Tolic, L., Shen, Y., Conrads, T. P., *et al*. (2002) An accurate mass tag strategy for quantitative and high-throughput proteome measurements. *Proteomics* **2**: 513–523.

Stanley, J. R., Adkins, J. N., Slysz, G. W., Monroe, M. E., Purvine, S. O., Karpievitch, Y. V., *et al*. (2011) A statistical method for assessing peptide identification confidence in accurate mass and time tag proteomics. *Anal Chem* **83**: 6135–6140.

Syed, K., Shale, K., Pagadala, N. S., and Tuszynski, J. (2014) Systematic identification and evolutionary analysis of catalytically versatile cytochrome P450 monooxygenase families enriched in model basidiomycete fungi. *PLoS One* **9**: e86683.

Vanden Wymelenberg, A., Gaskell, J., Mozuch, M., Splinter BonDurant, S., Sabat, G., Ralph, J., *et al*. (2011) Significant alteration of gene expression in wood decay fungi *Postia placenta* and *Phanerochaete chrysosporium* by plant species. *Appl Environ Microbiol* **77**: 4499–4507.

Supporting Information

Additional Supporting Information may be found in the online version of this article at the publisher's web-site:

Fig. S1. Helium Ion Microscope images of Norway spruce and silver birch tissue after growth of *D. squalens.* (A), (B) Transverse sections of non-inoculated spruce wood tissue. Transverse sections of spruce tissue after (C) 2 weeks and (D) 4 weeks cultivation of *D. squalens* showing the hyphal colonization of cell lumen and thinning of the spruce secondary cell walls. (E), (F) Transverse sections of non-inoculated birch wood tissue. Transverse sections of birch tissue after (G) 2 weeks and (H) 4 weeks cultivation of *D. squalens* revealing vessels colonized by fungal hyphae and erosion of birch cell wall structures. Arrows indicate fungal hyphae.

Fig. S2. Gel-state 2-D heteronuclear single quantum coherence (HSQC) nuclear magnetic resonance (NMR) spectra plots showing changes in the spruce and birch

wood after culturing for 4 weeks with *D. squalens.* The spectra are from the 'A' replicates from Table 1.

Fig. S3. Principal component analysis (PCA) of (A) expressed plant biomass degrading (PBD) CAZy (191 genes; > 10 FPKM in at least one condition) and (B) expressed genes (9,215 genes; > 10 FPKM in at least one condition) in the two- and four-week *D. squalens* cultures in spruce and birch. The PCA was performed with the $\log_2$ FPKM values (first increased by 0.01 to remove any zero values) using the PCA function from the FactoMineR package in R. W = week.

Fig. S4. Extracellular activities for the degradation of xylan and mannan from the two- and four-week *D. squalens* cultures in spruce and birch. (A) Xylose and xylobiose release from birchwood xylan and mannose and mannobiose release from carob galactomannan using each of the biological replicate extracellular filtrates from the two- and four-week birch or spruce cultures. Error bars represent standard errors of two technical replicates from the enzymatic assays. This data was presented in Fig. 3(A) as proportions of the combined sugars released from the two polysaccharides. (B) The relative amounts of sugars released from xylan and galactoglucomannan from the pooled extracellular filtrates from the three biological replicate cultures along with an accompanying graph showing the quantities of each of the individual sugars released. W = week.

Fig. S5. Heatmap showing the Pearson's correlation between the raw gene counts from the three biological replicates of the two- and four-week *D. squalens* cultures in spruce and birch. The libraries are ordered as groups of replicates. The cells containing the correlations between replicates have a purple border around them. W = week.

Table S1. Sugar composition of the spruce and birch wood as measured from acid hydrolysates from residues.

Table S2. Exo-proteome dataset of the two- and four-week *D. squalens* cultures in spruce and birch. (A) Overview of the exo-proteome dataset showing the total number of proteins identified, the proportion of identified proteins annotated with a putative signal peptide (SignalP) and the relative abundance of proteins annotated with a putative signal peptide in the exo-proteome in each replicate culture and (B) normalized abundances, fold changes and *p* values for exo-proteome dataset. Abbreviations: W = week, XC = xylanolytic CAZymes, MC = mannanolytic CAZymes, LME = lignin modifying enzymes and N/A = not applicable.

Table S3. RNAseq dataset from the two- and four-week (2w and 4w) *D. squalens* cultures in spruce and birch showing the FPKM value for each replicate, the mean and standard error of the FPKM for a condition and the DESeq fold changes and p_{adj} values. Various annotations for the Dicsqu464_1 genes are included. Abbreviations: W = week, XC = xylanolytic CAZymes, MC = mannanolytic CAZymes, LME = lignin modifying enzymes and N/A = not applicable.

Table S4. Transcript abundance from the two- and four-week *D. squalens* cultures in spruce and birch for genes putatively involved in carbon catabolic pathways of galactose, mannose, xylose and arabinose (sugars that differ in abundance between spruce and birch). The genes are listed as part of the pathways identified in ascomycetes as described in the review of Khosravi and colleagues (2015). The ortholog(s) in ascomycetes are also listed. W = week.

Table S5. Exo-metabolomics dataset. Abundance (peak area) of 64 identified metabolites from the two- and four-week *D. squalens* cultures in spruce and birch and non-inoculated controls. The same volume of extracted metabolites was analysed for each sample. W = week.